JOURNAL OF BACTERIOLOGY, Aug. 1997, p. 4664–4670 Vol. 179, No. 15
0021-9193/97/$04.00+0

The *Saccharomyces cerevisiae* Mevalonate Diphosphate Decarboxylase Is Essential for Viability, and a Single Leu-to-Pro Mutation in a Conserved Sequence Leads to Thermosensitivity

THIERRY BERGÈS,* DANIEL GUYONNET, AND FRANCIS KARST

Faculté des Sciences, Laboratoire de Génétique Physiologique et Moléculaire, Institut de Biologie Moléculaire et d'Ingénierie Génétique, Université de Poitiers, F-86022 Poitiers Cedex, France

Received 6 March 1997/Accepted 2 June 1997

The mevalonate diphosphate decarboxylase is an enzyme which converts mevalonate diphosphate to isopentenyl diphosphate, the building block of isoprenoids. We used the *Saccharomyces cerevisiae* temperature-sensitive mutant defective for mevalonate diphosphate decarboxylase previously described (C. Chambon, V. Ladevève, M. Servouse, L. Blanchard, C. Javelot, B. Vladescu, and F. Karst, Lipids 26:633–636, 1991) to characterize the mutated allele. We showed that a single change in a conserved amino acid accounts for the temperature-sensitive phenotype of the mutant. Complementation experiments were done both in the *erg19*-mutated background and in a strain in which the *ERG19* gene, which was shown to be an essential gene for yeast, was disrupted. Epitope tagging of the wild-type mevalonate diphosphate decarboxylase allowed us to isolate the enzyme in an active form by a versatile one-step immunoprecipitation procedure. Furthermore, during the course of this study, we observed that a high level of expression of the wild-type *ERG19* gene led to a lower sterol steady-state accumulation compared to that of a wild-type strain, suggesting that this enzyme may be a key enzyme in mevalonate pathway regulation.

The mevalonate (MVA) pathway provides the cell with numerous fundamental molecules called isoprenoids, including sterols, the side chain of ubiquinone, dolichol, prenyl groups of prenylated proteins such as *ras*, plant hormones, and aromatic compounds, etc (11, 14). For this reason, many groups have focused on this pathway, both as a potential target for inhibitors acting either as antifungal compounds in agriculture and medicine or as cellular antiproliferative agents and as a means for lowering serum cholesterol levels (for a review, see reference 20). For instance, simvastatin, an inhibitor of the 3-hydroxy-3-methylglutaryl–coenzyme A (HMG-CoA) reductase is used as a hypocholesterolemic agent and terbinafin, inhibitor of the fungal squalene epoxidase, and ketoconazole, inhibitor of the fungal lanosterol-14-demethylase, are well known antifungal agents and commonly used in human disease therapy.

Most of the structural genes coding for the enzymes involved in sterol biosynthesis have been cloned and characterized from many organisms, and regulation of this pathway in higher eucaryotes has been well documented (14). A substantial contribution to the cloning of these genes has come from the isolation of a collection of ergosterol auxotrophic mutants generated in the yeast *Saccharomyces cerevisiae* (17). Several sterol biosynthesis structural genes or cDNAs have been cloned by functional complementation of these mutants (13, 18, 21).

Of the enzymes of the MVA pathway, MVA diphosphate (MVA-PP) decarboxylase is one of the less well known. This enzyme converts MVA-PP into isopentenyl diphosphate (IPP), the building block of isoprenoids, and requires ATP and Mg^{2+} for its activity (8).

MVA-PP decarboxylase has been shown to be competitively inhibited by phenylalanine derivatives, such as phenylpyruvate, phenylacetate, and phenylalanine itself (9). Phenylacetate accumulation during fetal brain development in phenylketonuria results in severe brain damage leading to microcephaly and mental retardation (24). As the MVA-PP decarboxylase is an early enzyme in the MVA pathway, phenylacetate effects may be due to the lack of fundamental intermediary or end products of the MVA pathway. These observations have led to trials in using phenylacetate as an antiproliferative agent on malignant gliomas, a form of primary brain tumors (23). Recently Prasanna et al. (22) have shown that specific inhibition of the MVA-PP decarboxylase with phenylacetic acid and sodium salt (NaPA), when used together with lovastatin, a specific inhibitor of HMG-CoA reductase, could reverse the malignant phenotype of human glioblastoma cells.

Although a temperature-sensitive yeast strain deficient in MVA-PP decarboxylase activity was isolated and characterized some years ago (10), so far cloning by functional complementation of the enzyme's structural gene has failed, mainly because of the relatively high reversion rate of the *MN19-34* mutant deficient in MVA-PP decarboxylase.

Recently Toth and Huwyler (26) reported the isolation of the cDNAs encoding rat, human, and yeast MVA-PP decarboxylase (which they called MPD) with the help of peptide sequence data obtained from the enzyme purified from rat liver (27).

In this paper we report the cloning of the gene encoding the yeast MVA-PP decarboxylase by functional complementation of the yeast mutant isolated in our laboratory and we show that this gene is essential for yeast cell viability. We also report the cloning and sequencing of the mutated recessive allele. We have localized the mutation to a conserved amino acid. We show that this single change of a leucine to a proline is sufficient to confer a temperature-sensitive phenotype to the strain harboring this allele.

* Corresponding author. Mailing address: IBMIG, Laboratoire de Génétique Physiologique et Moléculaire, 40 avenue du Recteur Pineau, F-86022 Poitiers Cedex, France. Phone: (33) 0549-45-40-29. Fax: (33) 0549-45-35-03. E-mail: berges@hermes.univ-poitiers.fr.

MATERIALS AND METHODS

Cloning and characterization of the *ERG19* gene. The yeast genomic library was a generous gift from F. Lacroute. In this library, yeast genomic DNA

fragments partially digested with *Sau*3A are ligated into high-copy-number plasmid pFL44L (7). The gene marker used to select transformants is the *URA3* gene. This library was used to transform temperature-sensitive strain *MN19-34* (*MAT***a** *ura3 trp1*), which is deficient in MVA-PP decarboxylase activity and which was derived from original mutant strain *MNerg19* (10). Approximately 10^5 independent Ura^+ transformants were pooled and plated on selective medium at a nonpermissive temperature (36°C). One of the strains growing at 36°C showed plasmid-dependent growth and was kept for further analysis. This strain harbored a plasmid containing a genomic insert whose size was estimated to be about 6.5 kb. A unique *Sal*I site and a unique *Bgl*II site located approximately in the middle of the 6.5-kb genomic insert were used, in addition to restriction sites of high-copy-number plasmid pFL44L, to subclone the original insert. Two subclones corresponding to a *Sma*I-*Bgl*II restriction fragment of ~3 kb and a *Sal*I-*Sal*I restriction fragment of ~3 kb were subcloned in plasmid pFL44S (7) to generate, respectively, pTB1 and pTB2. These two plasmids were subsequently transformed into temperature-sensitive strain *MN19-34*. Only pTB2 reversed the phenotype of the mutated strain, i.e., allowing growth at 36°C. The insert contained in pTB2 was further partly deleted by using on one hand an *Xba*I site located both in the insert and in the multiple cloning site to generate pTB3 and on the other hand a *Pst*I site to generate pTB4. The complementing activity was restricted to the 1.94-kb *Pst*I-*Sal*I restriction fragment of pTB4, which was then fully sequenced.

Disruption of the *ERG19* gene. In order to inactivate the *ERG19* gene, two *Bgl*II restriction sites were generated by PCR. The sequences of the two oligonucleotides were 5′TTT*AGATCT*GGTGCTCACTGTCTGG3′ (195BG), which was designed to create a first *Bgl*II site at position 538 (from the *Pst*I site), 7 nucleotides upstream from the ATG start codon, and 5′ATTAGATCTTGAGT TGCAAAAGG3′ (193BG), which was designed to create a second *Bgl*II site at position 1620, 112 nucleotides upstream from the TAA stop codon. The pUC18-295 construct was used as a template for the PCRs. PCR product 1 (PCR1) of about 540 bp corresponding to the promoter part of the *ERG19* gene was obtained with universal M13 and 195BG primers. PCR product 2 (PCR2) of about 320 bp corresponding to the 3′ part of the *ERG19* gene was obtained with the reverse and the 193BG primers. PCR1 was digested with *Pst*I and *Bgl*II, and PCR2 was digested with *Bgl*II and *Sal*I. Both fragments were ligated with the pUC18 vector digested with *Pst*I and *Sal*I, generating the pUC18-Δ19 intermediary construct, in which most of the coding sequence of the *ERG19* gene is deleted.

The *TRP1* gene was prepared from the YDp-W plasmid as a 0.8-kb restriction fragment and ligated into pUC18-Δ19 cut with *Bgl*II and dephosphorylated, generating the pUC18-Δ19W plasmid. The pUC18-Δ19W plasmid was then cut with *Pst*I and *Sal*I in order to purify the 1.66-kb restriction fragment harboring the *erg19*::*TRP1* allele, which was subsequently transformed into the 5302 (*trp1*/*trp1 ura3*/*ura3*) diploid strain (19). Trp^+ transformants were then sporulated, and tetrads were dissected.

Epitope tagging of the MVA-PP decarboxylase. Two Z domains corresponding to the immunoglobulin G (IgG) binding domains of protein A from *Staphylococcus aureus* were fused in frame to the N terminus of the MVA-PP decarboxylase. The 1.1-kb *Bam*HI-*Sac*I restriction fragment corresponding to the *NOP1* promoter and to the two Z domains of protein A was prepared from the pProtA-NOP1 plasmid (5). In order to fuse in frame the coding sequence of the *ERG19* gene, we designed the PA19 oligonucleotide which contains a *Sac*I restriction site just downstream from the ATG codon (5′TTT*GAGCTC*GACC GTTTACACAGCATC3′). The *ERG19* gene was amplified by PCR with the PA19 and the reverse primers, with the pUC18-295 construct as the template. The 1.4-kb PCR product was then digested with *Sac*I and *Sal*I and ligated with the 1.1-kb *Bam*HI-*Sac*I fragment (*NOP1* promoter plus two Z domains) and the pFL44L plasmid cut with *Bam*HI and *Sal*I to generate the pPA295-1 plasmid. The same primers and the same procedure were used to clone the *erg19* mutated allele from the temperature-sensitive *MN19-34* strain (giving the pPA295ts-1 construct).

Each tagged gene was prepared as a 2.5-kb *Bam*HI-*Sal*I restriction fragment and cloned into the pRS316 single-copy plasmid giving the pPA295-2 (wild-type *ERG19*) and the pPA295ts-2 (*erg19* allele from the temperature-sensitive strain) constructs.

Immunoprecipitation of the tagged protein. Immunoprecipitation of the protein A fusion proteins was done as described by Bergès et al. (5) with some modifications. Cells were grown to saturation in selective medium (100 ml), washed with potassium phosphate buffer (0.1 M, pH 7.4), and eventually resuspended in potassium phosphate buffer (0.1 M, pH 7.4) containing 0.5 mM EDTA and 10 mM dithiothreitol. The cells were broken with glass beads, and the debris were eliminated by a short centrifugation at 3,000 × *g*. The homogenate was then centrifuged for 30 min at 12,000 × g at 4°C, and the amount of protein of the crude extract (in micrograms per milliliter) was estimated by performing the following calculation: $OD_{228.5} - OD_{234.5} \times 0.317 \times$ dilution factor (TOT fraction), where $OD_{228.5}$ is the optical density at 228.5 nm.

To 700 μl of potassium phosphate buffer (0.1 M, pH 7.4) 4 mg of protein A-Sepharose (Sigma) and 10 μg of rabbit IgG (whole molecule; Sigma) were added, and the mixture was incubated for 30 min. Unbound IgG was eliminated by washing with potassium phosphate buffer. To the pellet 700 μl of potassium phosphate buffer and 300 to 500 μg of protein of the crude extract were added, and the mixture was incubated at 4°C for 1.5 h. After a short centrifugation (3,000 × *g*, 2 min), the supernatant was kept (SUP fraction) and the pellet was washed three times with potassium phosphate buffer. The pellet was eventually resuspended in sodium dodecyl sulfate-polyacrylamide gel electrophoresis loading buffer.

MVA-PP decarboxylase activity determination. To assay the enzyme activity, a crude protein extract centrifuged at 12,000 × *g* was prepared as described above. To 200 μg of protein a mixture of 10 mM $MgCl_2$, 20 mM ATP, 0.5 mM NADPH, 1 mM glucose-6-phosphate, 2 U of glucose-6-phosphate dehydrogenase, and 23.5 μM [2-^{14}C]MVA (53 mCi/mmol) in potassium phosphate buffer (0.1 M, pH 7.4) was added, in a total volume of 200 μl.

Following a 40-min incubation at 37°C, 500 μg of cold carrier ergosterol, lanosterol, squalene, and squalene oxide was added. The mixture was gently saponified for 30 min at 42°C in the presence of methanolic KOH (10% final concentration) and extracted with heptane. The heptane phase was concentrated under vacuum, and the radioactivity of an aliquot was measured by liquid scintillation. The main fraction was then separated on Silica Gel G developed with dichloromethane. The distribution of radioactivity was determined with a Berthold 2382 thin-layer chromatography (TLC) scanner. To assay the activity of the immunoprecipitated protein, the same experiment was performed in the presence of the immobilized fusion protein immunoprecipitated under the conditions described above (200 μg of protein).

Sterol extraction and analysis. Sterol extraction was done essentially as described previously (16). Sterols were quantified by UV absorption (% 5,7 = $OD_{281.5}$ × volume of the heptanolic phase in milliliters × 396/11,500 × dry weight in milligrams, where %5,7 is the percentage of dry weight of the Δ5,7 sterols [sum of dry weight percentages for ergosterol and ergosta-5,7-dienol]), and the various species were analyzed by gas-liquid chromatography. The gas chromatograph (GC 6000; Carlo-Erba) was supplied with a flame-ionization detector and an on-column injector. The column was an RSL 150 (Altech) capillary. Cholesterol (Sigma) was used as the internal standard to determine relative retention times (in minutes), which were as follows: squalene, 0.72; cholesta-8,24-dienol (zymosterol), 1.06; ergosta-5,7,22-trienol (ergosterol), 1.09; ergosta-8,24(28)-dienol (fecosterol) and ergosta-8,14-dienol (ignosterol), 1.13; ergosta-8-enol, 1.14; ergosta-7,24(28)-dienol (episterol) and ergosta-5,7-dienol, 1.16; and 4,4,14-trimethylcholesta-8,24-dienol (lanosterol), 1.24.

RESULTS

Cloning and characterization of the *ERG19* gene. We have isolated a genomic DNA fragment able to reverse the temperature-sensitive phenotype of the *MN19-34* strain deficient in MVA-PP decarboxylase activity.

The insert size of the plasmid from the library (pDG295) carrying the complementing activity was estimated to be 6.5 kb. A limited restriction map was developed to permit the choice of convenient restriction sites for subcloning into high-copy-number plasmid pFL44S (7).

After several subcloning steps (Fig. 1; see Materials and Methods) the complementing activity was restricted to a 1.94-kb restriction fragment whose sequence was determined. Two head-to-head open reading frames (ORFs) were found on this insert: an incomplete ORF encoding 102 amino acids was identified by sequence comparison as the portion of the yeast *COQ2* gene coding for the N-terminal third of *para*-hydroxybenzoate polyprenyltransferase (3). The second ORF was complete and corresponds to the MVA-PP decarboxylase coding sequence which was reported during the course of our study (*MVD1* gene) (26).

Therefore, we confirmed that the gene able to complement the *MN19-34* mutant corresponds to the structural gene coding for the MVA-PP decarboxylase.

The *ERG19* gene is essential for viability. In order to inactivate the *ERG19* gene, we replaced most of the coding sequence with the *TRP1* gene after having generated convenient restriction sites by PCR. In this construct, the deletion includes the ATG start codon of *ERG19* and only the last 37 codons of the C-terminal part remain from the coding sequence. The deleted *erg19*::*TRP1* gene was then inserted by homologous recombination into the 5302 (*trp1*/*trp1 ura3*/*ura3*) diploid strain (19). Tetrad dissection resulted in a 2:2 segregation of the viability (Fig. 1), the two viable spores being auxotrophs for tryptophan (data not shown). Moreover, the pTB4 plasmid was transformed into an *ERG19*/*erg19*::*TRP1 trp1*/*trp1 ura3*/*ura3*

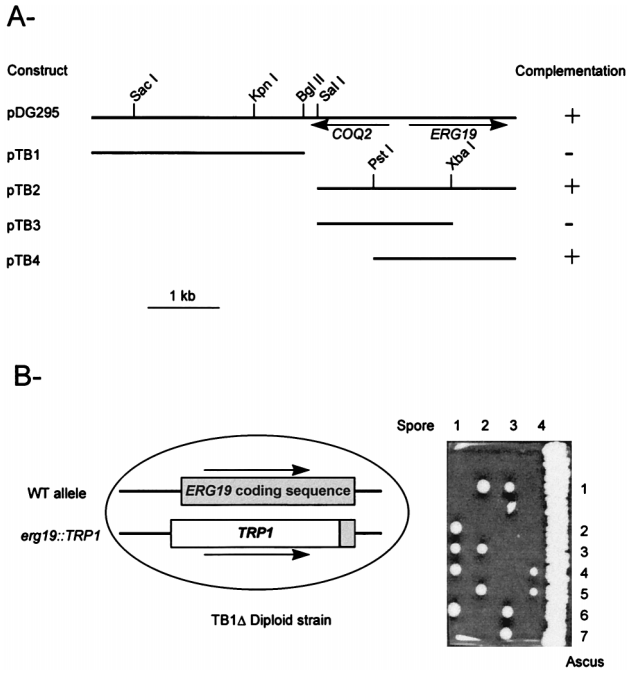

FIG. 1. Subcloning steps to locate the *ERG19* gene (A) and to perform gene disruption (B). The pDG295 plasmid represents the original genomic clone isolated from the library. The various restriction fragments were subcloned into high-copy-number plasmid pFL44S (see Materials and Methods), and each construct was assayed for complementation of the *MN19-34* strain. Tetrad dissection was carried out on YPD. Each viable spore was shown to be prototrophic for tryptophan. In panel B, the arrows indicate the transcription orientation. WT, wild type.

diploid strain (TB1Δ), sporulation was induced, and the haploid progeny was analyzed. Haploid Trp^+ Ura^+ strains could be obtained but did not survive on 5-FOA-containing medium (data not shown), confirming that the *ERG19* gene is not dispensable for viability in yeast.

Epitope tagging of the protein encoded by *ERG19*. In order to immunoprecipitate the protein encoded by the *ERG19* gene and to assay the MVA-PP decarboxylase activity in vitro, we chose to tag the protein with the IgG binding domain of protein A from *S. aureus*. This strategy has already been used several times to allow either immunoprecipitation and affinity purification or immunolocalization of a protein of interest or to compensate for the lack of specific antibodies directed against the protein (15, 25, 29). The epitope domain we have used consists of the two repetitive IgG binding domains (Z-Z) of about 15,000 Da which were fused to the N terminus of the amino acid sequence deduced from the *ERG19* gene. In our construct, transcription of the chimeric gene is driven by the yeast *NOP1* promoter. *NOP1* is a housekeeping gene encoding the yeast nucleolar protein fibrillarin, a very abundant protein involved in ribosome biogenesis and highly conserved throughout evolution. Although this promoter is not as strong as other well-known promoters like the *PGK* or *ADH1* promoters, it is recognized as a constitutive and relatively strong promoter. The chimeric gene was inserted into a high-copy-number plasmid (pFL44L). The resulting plasmid, pPA295-1, was transformed into the *MN19-34* strain, and replica plating of the Ura^+ transformants at a nonpermissive temperature showed that the fusion protein fully complements the temperature-sensitive phenotype (Fig. 2).

A crude protein extract was prepared from this strain, and the fusion protein could be efficiently detected on a Western blot with PAP antibodies (peroxidase-antiperoxidase rabbit IgG). The observed molecular mass of the fusion protein (~60,000 Da) is consistent with the predicted molecular mass of the chimeric ProtA-ERG19 protein deduced from the sequence of the gene (44,000 + 15,000 Da) (Fig. 2).

The pPA295-1 construct was transformed into the diploid strain in which one copy of the *ERG19* gene was disrupted (TB1Δ strain; *ura3*/*ura3 trp1*/*trp1 ERG19*/*erg19*::*TRP1*). The haploid Ura^+ Trp^+ progeny was selected after sporulation; it carried both the *erg19*::*TRP1* allele and plasmid pPA295-1.

The chimeric gene expressing the ProtA-ERG19 fusion protein was also cloned into single-copy vector pRS316, giving plasmid pPA295-2. This construct was transformed into the *MN19-34* temperature-sensitive strain. The transformed strain grew normally at 36°C, showing that the fusion protein produced from a single-copy plasmid fully complements the mutation (data not shown). The construct was also transformed into the TB1Δ (*ERG19*/*erg19*::*TRP1*) diploid strain to obtain a strain in which the only MVA-PP decarboxylase was the tagged protein. After sporulation, viable Ura^+ Trp^+ progeny could be obtained, confirming that the fusion protein was functional (Fig. 4B, lane 2). A Western blot analysis showed that the level of production of the fusion protein from the single-copy vector was severely reduced (data not shown).

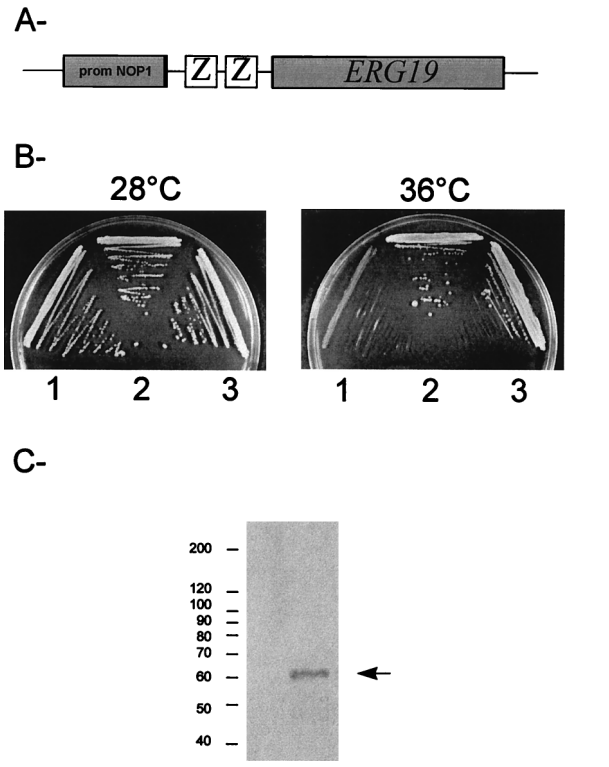

FIG. 2. Expression of *ERG19* tagged with IgG binding domains of protein A in yeast. (A) Schematic drawing of the ProtA-ERG19 construct. Two IgG binding domains (Z) were fused to the N terminus of the *ERG19* coding sequence and cloned into the pFL44S plasmid (see Materials and Methods). prom, promoter. (B) The pPA295-1 construct with the fusion protein (3) was transformed into the *MN19-34* strain deficient in MVA-PP decarboxylase, and growth was assayed on YPD at 28°C and at a nonpermissive temperature (36°C). Controls were the untransformed *MN19-34* strain (1) and the *MN19-34* strain transformed with the untagged Erg19p protein from pTB4 (2). (C) Immunoblot analysis. A crude protein extract was prepared from the *MN19-34* strain transformed with the pPA295-1 construct and was analyzed by Western blotting. The fusion protein (arrow) was detected with PAP IgG.

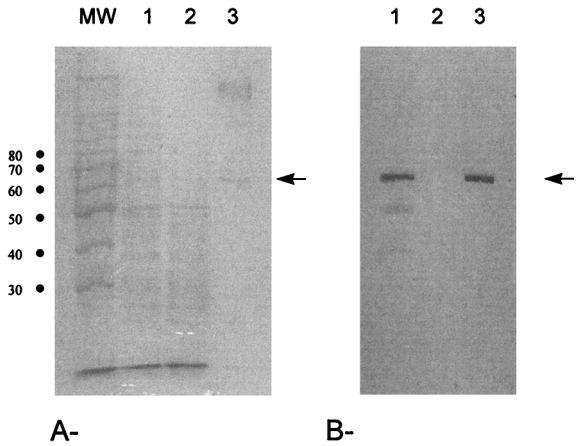

FIG. 3. Immunoprecipitation of tagged Erg19p. A crude protein extract was prepared from a haploid strain carrying the *erg19*::*TRP1* disrupted allele transformed with the pPA295-1 plasmid expressing the ProtA-Erg19p fusion protein. The proteins (500 μg) were incubated with IgG coupled to ProtA-Sepharose for 1 h at 4°C. After precipitation, samples corresponding to the supernatant (SUP fraction) (2) and to the pellet (3) were loaded on a sodium dodecyl sulfate-polyacrylamide gel electrophoresis gel and analyzed by Coomassie staining (A) and by Western blotting (B) using PAP antibodies to detect the fusion protein (arrow). The control lane (TOT fraction) (1) corresponds to a sample of the crude extract before immunoprecipitation. Approximately the same amount of protein was loaded in each lane. Standards are in kilodaltons.

TABLE 1. Conversion of radiolabeled MVA into nonsaponifiable lipids in crude protein extracts

Strain	Amt of MVA[a] (nmol)	% Reaction product[b]			
		Squalene	Squalene oxide	Lanosterol	Baseline
FL100	0.83	93	2	2	3
erg19::*TRP1*[c]	0.42	74	2	5	18
MN19-34	0.07	67	9	ND[d]	17
MN19-34 + IP[e]	0.52	85	5	4	6

[a] Amount of [2-^{14}C]MVA converted into nonsaponifiable lipids.
[b] Percent total nonsaponifiable lipids loaded. Separation was by TLC, and radioactivity measurements were performed with a Berthold 2382 TLC analyzer.
[c] Strain carrying gene *erg19*::*TRP1* (pPA295-1; multicopy, wild-type strain).
[d] ND, not detected.
[e] IP, immunoprecipitated protein.

A whole-cell extract (centrifuged at 12,000 × *g*) was prepared under nondenaturing conditions from the strain overproducing the ProtA-ERG19 fusion protein (pPA295-1 plasmid). Nonspecific rabbit IgGs preincubated with protein A-Sepharose were added to the protein extract and incubated for 90 min at 4°C. After sedimentation of the resin, the proteins from the extract, from the supernatant, and from the immunoprecipitation pellet were analyzed both by Coomassie staining and by Western blot analysis using PAP antibodies. The result of the experiment shows that more than 90% of the fusion protein from the crude protein extract was retained in the pellet (Fig. 3). Moreover, the fusion protein was significantly abundant in the pellet since it was visible by Coomassie staining, and besides the heavy chains of the IgGs, it was the only protein detected in the immunoprecipitated pellet.

To check whether the enzyme prepared under these conditions was active, we first showed that a crude protein extract (centrifuged at 12,000 × *g*) prepared from the *MN19-34* mutant and incubated with radiolabeled MVA produced very small amounts of sterols (1.6% MVA converted) compared to those produced by extract from a wild-type strain (17% of MVA converted) or to those produced by extract from a strain carrying *erg19::TRP1* complemented with pPA295-2 (wild-type *ERG19*; monocopy) (9% of MVA converted), confirming the leaky phenotype of this mutant (Table 1). When the immunoprecipitated fusion protein was added to such an MVA-PP decarboxylase-deficient mixture, a significant amount of sterols was produced (11% of MVA converted), which could be separated by TLC and identified (Table 1). These results showed that the MVA pathway could be restored by the addition of the immunoprecipitated MVA-PP decarboxylase.

Overexpression of the *ERG19* gene impairs the MVA pathway. Total sterols were extracted from a control wild-type strain (FL100) grown in complete medium yeast-peptone-dextrose (YPD), from the *MN19-34* strain grown at a permissive temperature in YPD without addition of exogenous ergosterol, from the strain carrying the disrupted *erg19*::*TRP1* gene complemented with the *ERG19* gene on a high-copy-number plasmid (pTB4), and from the same strain transformed with the pPA295-2 plasmid (tagged *ERG19*, monocopy). The sterols of the above-mentioned strains were analyzed by UV absorption and gas chromatography (GC) (see Materials and Methods). The results obtained from three independent experiments are shown in Table 2.

While the mean value for the percentage of dry weight of the Δ5,7 sterols (sum of ergosterol and ergosta-5,7-dienol) for the wild-type strain is around 0.80%, the *MN19-34* strain produced a significantly smaller amount of sterols (0.25%). The GC analysis revealed that for the mutant strain, only ergosterol is significantly detected. This is in contrast to the wild-type strain, for which this sterol represents only about 56%. Therefore, it appears that the *MN19-34* mutant strain produces a 6-fold-smaller sterol amount than the corresponding wild-type isogenic strain. It should be noted that under these conditions the *MN19-34* strain is not sterol auxotrophic at 28°C.

The tagged version of *ERG19* under the control of *NOP1* promoter, carried on a single-copy vector (pPA295-2), led to a wild-type-like ergosterol production level of 0.86% for the strain carrying *erg19*::*TRP1*. In contrast, when the wild-type *ERG19* gene is carried on a multicopy vector (pTB4) in the same strain, the ergosterol level remains low (0.38%, i.e., about half that of the wild type). The GC analysis also showed that the sterol biosynthesis intermediates are also at lower levels than those associated with the wild-type strain.

This result suggests that the high level of MVA-PP decarboxylase gene expression may be at the basis of the small ergosterol amount produced by the strain carrying *erg19*::*TRP1* (pTB4).

Cloning of the *erg19* allele from the temperature-sensitive strain. A PCR product corresponding to the *erg19* allele coding sequence was obtained from the *MN19-34* temperature-sensitive strain by using oligonucleotides which were designed to allow further epitope tagging of this allele. The chimeric *ProtA-erg19ts* allele construction was done both in high-copy-number plasmid pFL44L and in single-copy plasmid pRS316, generating, respectively, the pPA295ts-1 (multicopy) and the pPA295ts-2 (monocopy) plasmids. Two independent PCR products were also cloned in parallel in pUC18 for sequencing. In addition, the *erg19* coding sequence was cloned from expression vector pPA295ts-2 and its sequence was determined.

In all cases, sequencing of the *erg19* allele coding sequence allowed us to find a single (T→C) point mutation at position 779 (from the *Pst*I site), resulting in the replacement of leucine 79 by a proline (L79P).

The pPA295ts-1 and the pPA295ts-2 plasmids were transformed into the *MN19-34* strain, and the Ura$^+$ transformants were restreaked on complete medium at 36°C. The transfor-

TABLE 2. Comparative sterol compositions of various strains

Strain	% 5,7[a]	% Sterol ± SD				
		Zymosterol[b]	Ergosterol	Ergost-8-enol	Ergosta-5,7-dienol	Lanosterol
FL100	0.80 ± 0.06	16 ± 2	56 ± 6	10 ± 5	12 ± 1	6 ± 4
MN19-34	0.25 ± 0.02	ND[c]	99 ± 1	ND	ND	1 ± 1
erg19::*TRP1* (pTB4)[d]	0.38 ± 0.02	12.0 ± 0.6	75 ± 2	ND	8 ± 2	5 ± 1
erg19::*TRP1* (pPA295-2)[e]	0.86 ± 0.09	22 ± 3	58 ± 3	2 ± 1	12 ± 2	4 ± 1

[a] % 5,7 is the percentage of dry weight of the Δ5,7 sterols (sum of the dry weight percentages for ergosterol and ergosta-5,7-dienol). The equation for % 5,7 is given in Materials and Methods.
[b] Values determined by GC.
[c] ND, not detected.
[d] Multicopy.
[e] Monocopy.

mants obtained with pPA295ts-1 could grow at 36°C to the same extent as a wild-type strain, but the transformants obtained with single-copy plasmid pPA295-2 could not complement the temperature-sensitive phenotype (data not shown). We then transformed both plasmids into the TB1Δ strain. The Ura^+ transformants were sporulated, and viable haploid Ura^+ Trp^+ strains could be recovered. The strain carrying the *erg19*::*TRP1* gene produced from wild-type *ERG19* (pPA295-2; monocopy) and that carrying the *erg19*::*TRP1* gene produced from mutated *erg19* (pPA295ts-2; monocopy) were restreaked at 36°C (Fig. 4B). Only the strain with the wild-type allele could grow at 36°C, showing that the *erg19* allele from the mutant strain alone is responsible for the temperature-sensitive phenotype of the *MN19-34* strain.

A Western blot analysis confirmed that the fusion protein is expressed, with an apparent molecular mass identical to that of the protein produced from the wild-type *ERG19* (Fig. 4C), although the doubling time at a permissive temperature is slightly enhanced (by a factor of 1.2), suggesting that the enzyme for the *MN19-34* mutant, even at the permissive temperature, is slightly less active than its wild-type counterpart. When the proteins were prepared after 6-h growth at 36°C, no difference could be detected (data not shown). We therefore concluded that the defect in the mutant strain is not due to a higher turnover of the messenger RNA of *ERG19* or of the protein but that the point mutation could affect directly the catalytic site or the interaction domain necessary for homodimerization. It is important to point out that this Leu-79 residue is one of the residues conserved between the yeast, human (26), and *Arabidopsis thaliana* MVA-PP decarboxylases (11a).

DISCUSSION

This paper reports the cloning by functional complementation of the yeast gene encoding MVA-PP decarboxylase. Evidence is given to show that mutant strain *MN19-34* (10) bears a defect in the MVA-PP decarboxylase structural gene.

The genomic sequence of *ERG19* is identical to that of the cDNA, as reported by Toth and Huwyler (26). As reported by these authors, *ERG19* and *COQ2* (encoding *para*-hydroxybenzoate polyprenyl transferase) are transcribed from divergent promoters, the two ORFs being separated by only 250 bp. This is significantly below the average length since the data from the yeast genome sequence indicate that divergent ORFs are on average about 600 nucleotides apart (12). Yet the possible physiological significance of this peculiarity has not been studied, although it is tempting to speculate that sharing a short promoter area might be a way to coregulate related pathways. Another noticeable feature of the *ERG19* gene is the unusually long 3′-untranslated region (UTR) of its mRNA (about 600 nucleotides) as reported by Toth and Huwyler (26). This result, obtained from the cDNA isolated by these authors, is consistent with the yeast genome sequencing data. Again, the aver-

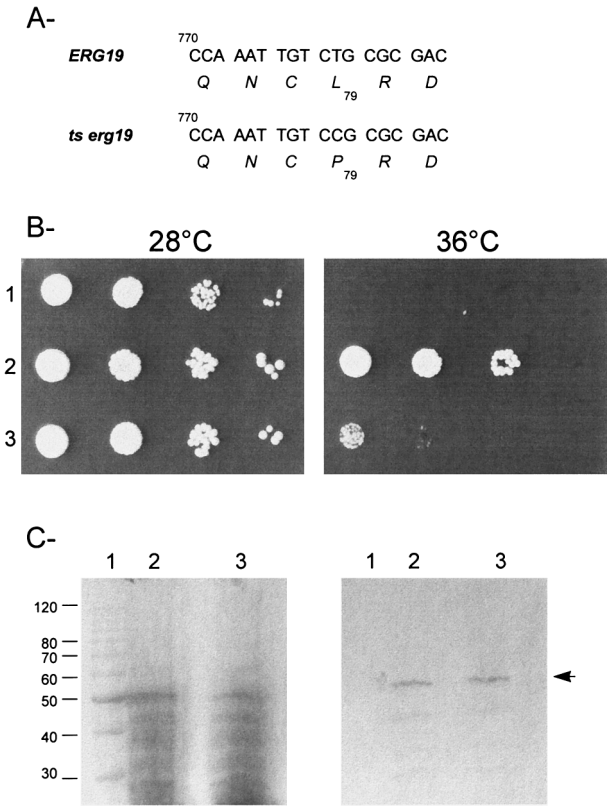

FIG. 4. The mutated *erg19* allele corresponds to a point mutation leading to thermosensitivity. (A) Sequence comparison of the *erg19* allele cloned by PCR from the temperature-sensitive *MN19-34* strain with the wild-type allele showing the T→C point mutation which changes the leucine 79 to a proline. (B) Dilution series showing the growth of the strain carrying *erg19*::*TRP1*, which contains monocopy plasmid pRS316 harboring the wild-type *ERG19* allele tagged with protein A (pPA295-2 plasmid) (lane 2) or harboring the mutated *erg19* allele tagged with protein A (pPA295ts-2 plasmid) (lane 3). Growth was assayed at 28 and 36°C on YPD. The *MN19-34* thermosensitive strain is shown as a control (lane 1). (C) Immunoblot analysis. Crude protein extracts were prepared from the strain carrying the *erg19*::*TRP1* gene produced from wild-type *ERG19* (pPA295-2; monocopy) (lane 2) and from that carrying the *erg19*::*TRP1* gene produced from the *erg19* mutated allele (pPA295ts-2; monocopy) (lane 3). The fusion protein (arrow) was detected with PAP IgG. A Coomassie-stained gel run in parallel is shown as a control for the amount of total protein loaded. Protein standards (lane 1) are in kilodaltons.

age for the 3′ UTRs of all yeast potential genes is around 160 nucleotides (12). In all our expression vectors, except for the original genomic clone (pDG295, Fig. 1), more than half of this region is truncated (~150 nucleotides of the original 3′ UTR are left in the pPA295 constructs), without an effect on complementation. The significance of this long 3′ UTR of the MVA-PP decarboxylase mRNA has not been determined.

The results presented here show that MVA-PP decarboxylase gene disruption is lethal to yeast. This result was expected, since ergosterol is not the unique end product of the MVA pathway and since yeast cells are impermeable to organic pyrophosphates and therefore cannot be supplemented with IPP, the product of MVA-PP decarboxylase. A similar result has been described for MVA kinase (21), phosphomevalonate kinase (28), IPP isomerase (1), and farnesyl diphosphate (FPP) synthase (2, 6) gene disruptions, showing that they are essential genes. However, before this study, one could not exclude the presence of a second gene for MVA-PP decarboxylase, as is the case for HMG-CoA reductase (4). Indeed, only one mutant (*MNerg19*) defective in MVA-PP decarboxylase has been described for yeast. This mutant exhibits a temperature-sensitive phenotype, and it could be speculated that this phenotype was the consequence of gene inactivation rather than of a leaky mutation.

Surprisingly, the overexpression of the wild-type *ERG19* gene leads to low sterol content for a yeast with a disrupted *ERG19* gene. One way to account for this result would be to argue that MVA-PP decarboxylase is a limiting enzyme in the sterol pathway in yeast and that overexpression results in an accumulation of IPP, geranyl diphosphate, or FPP that could feed back to the MVA kinase and/or the HMG-CoA reductase. This strain was nevertheless able to grow at any temperature, but the colonies were heterogeneous in size, suggesting that growth is somehow impaired.

We show that the mutated gene presents a leucine-to-proline mutation in the sequence of the MVA-PP decarboxylase leading to a temperature-sensitive phenotype of the strain harboring only the mutated copy. This mutation lies in a motif in which this leucine residue is conserved between yeast, rice, *A. thaliana*, rat, and human MVA-PP decarboxylase sequences that have been described so far (11a, 26). Considering that the level of production of the enzyme is not drastically reduced at a permissive temperature while the generation time is slightly increased, one could hypothesize that the activity of the enzyme itself is affected by the leucine-to-proline mutation, either because of a conformational change enhanced at high temperature or because of a modification in the catalytic site of the enzyme. Alternatively, this mutation could also affect a domain involved in the homodimerization of this enzyme. The oligomeric state of the yeast MVA-PP decarboxylase has not been studied so far, but it is known that the chicken liver MVA-PP decarboxylase is a dimer of identical subunits (8), and it has been shown recently that the native rat liver enzyme is also a homodimer (27). The use of our tagged versions of both the wild-type and the mutated enzymes prepared in native conditions at permissive and nonpermissive temperatures may help to check these hypotheses.

As an alternative approach to a fastidious enzyme purification procedure from yeast or to heterologous production of the enzyme in *Escherichia coli*, we used a method to isolate the enzyme in a single-step procedure with the help of a tag. The results presented here show that this procedure is versatile and very efficient, since more than 90% of the tagged protein could be depleted from a crude protein extract. Because the substrate of this enzyme, MVA-PP, was not readily available, we chose to assay the activity of the immunoprecipitated MVA-PP decarboxylase indirectly, i.e., by checking the ability to restore a functional MVA pathway leading to sterols (squalene, squalene oxide, and lanosterol) when radiolabeled MVA was incubated with an otherwise nonfunctional, MVA-PP decarboxylase-deficient protein extract. Although it is obvious that this assay cannot be used for enzyme biochemical parameter determination, this experiment showed at least that the tagged MVA-PP decarboxylase had been isolated in an active form in the immunoprecipitation procedure. Therefore, this enzyme preparation procedure should allow researchers to assay MVA-PP decarboxylase activity in vitro under various conditions when the enzyme is prepared in native conditions from yeast and also to test the activity of its mutant counterpart. This study may help in the design of new inhibitors of this key enzyme or in the study of the structural and functional relationships with in vitro-mutagenized *ERG19*.

ACKNOWLEDGMENTS

We thank Johann Joets for helpful advice for the GC analysis and the various members of the laboratory for helpful discussions during the course of this work. We are grateful to Randy Worobo and Mathieu Régnacq for critically reading the manuscript. Ed Hurt (University of Heidelberg) is acknowledged for the gift of the pRS316 plasmid.

This work was supported by grants from GREG/INRA (no. 9/95) and from the French Ministry of National Education and Research.

REFERENCES

1. **Anderson, M. S., M. Muehlbacher, I. P. Street, J. Proffit, and C. D. Poulter.** 1989. Isopentenyl diphosphate:dimethylallyl diphosphate isomerase. An improved purification of the enzyme and isolation of the gene from *Saccharomyces cerevisiae*. J. Biol. Chem. **264:**19169–19175.
2. **Anderson, M. S., J. G. Yarger, C. L. Burck, and C. D. Poulter.** 1989. Farnesyl diphosphate synthetase. Molecular cloning, sequence and expression of an essential gene from *Saccharomyces cerevisiae*. J. Biol. Chem. **264:**19176–19184.
3. **Ashby, M. N., S. Y. Kutsunai, S. Ackerman, A. Tzagoloff, and P. A. Edwards.** 1992. *COQ2* is a candidate for the structural gene encoding *para*-hydroxybenzoate:polyprenyltransferase. J. Biol. Chem. **267:**4128–4136.
4. **Basson, M. E., M. Thorsness, and J. Rine.** 1986. *Saccharomyces cerevisiae* contains two functional genes encoding 3-hydroxy-3-methylglutaryl-coenzyme A reductase. Proc. Natl. Acad. Sci. USA **83:**5563–5567.
5. **Bergès, T., E. Petfalski, D. Tollervey, and E. C. Hurt.** 1994. Synthetic lethality with fibrillarin identifies NOP77p, a nucleolar protein required for pre-rRNA processing and modification. EMBO J. **13:**3136–3148.
6. **Blanchard, L., and F. Karst.** 1993. Characterization of a lysine-to-glutamic acid mutation in a conservative sequence of farnesyl diphosphate synthase from *Saccharomyces cerevisiae*. Gene **125:**185–189.
7. **Bonneau, N., O. Ozier-Kalogeropoulos, G. Li, M. Labouesse, L. Minvielle-Sebastia, and F. Lacroute.** 1991. A family of low and high copy replicative, integrative and single-stranded *S. cerevisiae*/*E. coli* shuttle vectors. Yeast **7:**609–615.
8. **Cardemil, E., and A. M. Jabalquinto.** 1985. Mevalonate 5-pyrophosphate decarboxylase from chicken liver. Methods Enzymol. **110:**86–92.
9. **Castillo, M., M. Martinez-Cayuela, M. F. Zafra, and E. Garcia-Peregrin.** 1991. Effect of phenylalanine derivatives on the main regulatory enzymes of hepatic cholesterogenesis. Mol. Cell. Biochem. **105:**21–25.
10. **Chambon, C., V. Ladevèze, M. Servouse, L. Blanchard, C. Javelot, B. Vladescu, and F. Karst.** 1991. Sterol pathway in yeast. Identification and properties of mutant strains defective in mevalonate diphosphate decarboxylase and farnesyl diphosphate synthetase. Lipids **26:**633–636.
11. **Chappell, J.** 1995. Biochemistry and molecular biology of the isoprenoid biosynthetic pathway in plants. Annu. Rev. Plant Physiol. Plant Mol. Biol. **46:**521–547.

11a. **Cordier, H.** Unpublished data.

12. **Dujon, B.** 1996. The yeast genome project: what did we learn? Trends Genet. **12:**263–270.
13. **Fegueur, M., L. Richard, A. D. Charles, and F. Karst.** 1991. Isolation and primary structure of the *ERG9* gene of *Saccharomyces cerevisiae* encoding squalene synthase. Curr. Genet. **20:**365–372.
14. **Goldstein, J. L., and M. S. Brown.** 1990. Regulation of the mevalonate pathway. Nature **343:**425–430.
15. **Grandi, P., V. Doye, and E. C. Hurt.** 1993. Purification of NSP1 reveals complex formation with 'GLFG' nucleoporins and a novel nuclear pore protein NIC96. EMBO J. **12:**3061–3071.
16. **Joets, J., D. Pousset, C. Marcireau, and F. Karst.** 1996. Characterization of the *Saccharomyces cerevisiae FMS1* gene related to *Candida albicans* corti-

costeroid-binding protein 1. Curr. Genet. **30:**115–120.
17. **Karst, F., and F. Lacroute.** 1973. Isolation of pleiotropic yeast mutants requiring ergosterol for growth. Biochem. Biophys. Res. Commun. **52:**741–747.
18. **Lees, N. D., B. Skaggs, D. R. Kirsh, and M. Bard.** 1995. Cloning of the late genes in the ergosterol biosynthetic pathway of *Saccharomyces cerevisiae*. Lipids **30:**221–226.
19. **Marcireau, C., D. Guyonnet, and F. Karst.** 1992. Construction and growth properties of a yeast strain defective in sterol 14-reductase. Curr. Genet. **22:**267–272.
20. **Mercer, E. I.** 1993. Inhibitors of sterol biosynthesis and their applications. Prog. Lipid Res. **32:**357–416.
21. **Oulmouden, A., and A. Karst.** 1991. Nucleotide sequence of the *ERG12* gene of *Saccharomyces cerevisiae* encoding mevalonate kinase. Curr. Genet. **19:**9–14.
22. **Prasanna, P., A. Thibault, L. Liu, and D. Samid.** 1996. Lipid metabolism as a target for brain therapy: synergistic activity of lovastatin and sodium phenylacetate against human glioma cells. J. Neurochem. **66:**710–716.
23. **Samid, D., Z. Ram, W. R. Hudgins, S. Shacks, L. Liu, S. Walbridge, E. Oldfield, and C. E. Myers.** 1994. Selective activity of phenylacetate against malignant gliomas: resemblance to fetal brain damage in phenylketonuria. Cancer Res. **54:**891–895.
24. **Scriver, C. R., and C. L. Clow.** 1980. Phenylketonuria: epitome of human biochemical genetics. N. Engl. J. Med. **303:**1394–1400.
25. **Stirling, D. A., A. Petrie, D. J. Pulford, D. T. W. Paterson, and M. J. R. Stark.** 1992. Protein A-calmodulin fusions: a novel approach for investigating calmodulin function in yeast. Mol. Microbiol. **6:**703–713.
26. **Toth, M. J., and L. Huwyler.** 1996. Molecular cloning and expression of the cDNAs encoding human and yeast mevalonate pyrophosphate decarboxylase. J. Biol. Chem. **271:**7895–7898.
27. **Toth, M. J., L. Huwyler, and J. Park.** 1996. Purification of rat liver mevalonate pyrophosphate decarboxylase. Prep. Biochem. Biotechnol. **26:**47–51.
28. **Tsay, Y. H., and G. W. Robinson.** 1991. Cloning and characterization of *ERG8*, an essential gene of *Saccharomyces cerevisiae* that encodes phosphomevalonate kinase. Mol. Cell. Biol. **11:**620–631.
29. **Wimmer, C., V. Doye, P. Grandi, U. Nehrbass, and E. C. Hurt.** 1992. A new subclass of nucleoporins that functionally interacts with nuclear pore protein NSP1. EMBO J. **11:**5051–5061.